energies

MDPI

Article

The Fractured Permian Reservoir and Its Significance in the Gas Exploitation in the Sichuan Basin, China

Xin Luo [1], Siqi Chen [1], Jiawei Liu [2], Fei Li [3], Liang Feng [1], Siyao Li [2], Yonghong Wu [1], Guanghui Wu [2,*] and Bin Luo [1,3,*]

[1] Chongqing Division, PetroChina Southwest Oil & Gasfield Company, Chongqing 400707, China
[2] School of Geoscience and Technology, Southwest Petroleum University, Chengdu 610500, China
[3] PetroChina Southwest Oil & Gasfield Company, Chengdu 610051, China
* Correspondence: wugh@swpu.edu.cn (G.W.); lb2001@petrochina.com.cn (B.L.)

Abstract: Large gas reserves have been found in the Permian platform margin of the Kaijiang-Liangping area of the Sichuan Basin in SW China. They are assumed to be a widely developed reef–shoal reservoir. However, the tight matrix reservoir cannot support high gas production using conventional development technology at deep subsurface. In this contribution, we analyze the fractured reservoirs along the strike-slip fault zones using the compiled data of cores, well logging, and production data, and provide a seismic description. It was shown that the fractures and their dissolution developed along the strike-slip fault zones. The porosity and permeability of the fractured reservoir could increase by more than one and 1–2 orders of magnitude, respectively. The seismic anisotropic energy found in the steerable pyramid process suggests that fractured reservoirs have a strong heterogeneity, with a localized fault damage zone. This fracturing has both positive and negative effects, showing varied reservoir parameters in the fault damage zone. The development pattern should adopt a non-uniform well pattern, in order to target the localized "sweet spot" of the fractures in these deep tight matrix reservoirs.

Keywords: tight matrix reservoir; strike-slip fault; fractured reservoir; seismic reservoir description; deep gas exploitation; Sichuan basin

check for updates

Citation: Luo, X.; Chen, S.; Liu, J.; Li, F.; Feng, L.; Li, S.; Wu, Y.; Wu, G.; Luo, B. The Fractured Permian Reservoir and Its Significance in the Gas Exploitation in the Sichuan Basin, China. *Energies* **2023**, *16*, 1968. https://doi.org/10.3390/en16041968

Academic Editor: Xinpu Shen

Received: 30 December 2022
Revised: 6 February 2023
Accepted: 9 February 2023
Published: 16 February 2023

Copyright: © 2023 by the authors. Licensee MDPI, Basel, Switzerland. This article is an open access article distributed under the terms and conditions of the Creative Commons Attribution (CC BY) license (https://creativecommons.org/licenses/by/4.0/).

1. Introduction

Carbonate oil/gas resources are one of the major exploitation domains in the petroleum industry [1–3]. Considering the low porosity and permeability of deep (>4500 m) matrix reservoirs, fractured reservoirs have become more important in deep oil/gas exploitation [3–7]. The permeability and porosity of fractured reservoirs can be increased by more than 1–3 orders of magnitude and 20%, respectively [6–9]. Furthermore, a heterogeneous conductive fracture network plays an important role in oil/gas production and recovery [10–13]. In this way, description and characterization of fracture networks is a fundamental challenge in oil/gas exploitation. Generally, a fractured reservoir is described using seismic methods that examine the deep subsurface [14–16], whereas identification of the highly heterogeneous small-scale fracture network is generally beyond seismic resolution at deep subsurface [6,7]. In this context, the geological description and modeling of fractured reservoirs is of significant importance for deep oil/gas exploitation.

Large gas resources have been found in the Ediacaran-Triassic carbonate formation in Sichuan Basin, NW China [17]. Recently, some large carbonate gas fields have been found along the Permian-Triassic platform margin in the Kaijiang-Liangping area [18,19]. This carbonate reservoir is generally considered to be a reef–shoal facies-controlled reservoir modeled along the carbonate platform margins [18–22]. A matrix reservoir was well developed in the high-energy reef–shoal bodies and was favorable for the dissolution of meteoric and burial environments [20–22]. This contrasts with matrix reservoirs, which

generally have extremely low porosity (<4%) and permeability (<1 mD) and low production, which is expected in a tight reservoir. Generally, conventional exploitation technology do not allow a high level of gas production from the tight reservoirs. To overcome this challenge, a reservoir seismic description, horizontal well drilling, and large-scale acid-fracturing were carried out in the reef-shoal reservoirs. Although the gas production increased to a large extent, there are still many wells with low production in the deep tight reservoirs. There are several NW-trending strike-slip faults along the platform margins [23]. The steerable pyramid method was used to describe the carbonate fault damage zone, which could enhance the gas production of the carbonate reservoirs [23]. However, there is little information from cores and logging data available to characterize the fractured reservoirs along the strike-slip fault zones. This has constrained the optimization of gas production and recovery in these deep tight reservoirs.

In order to enhance gas production and recovery, we described the fractured reservoirs using core and logging data and made a comparison with the matrix reservoir. Furthermore, we produced a description of fractured reservoirs and advanced the knowledge of horizontal wells across strike-slip fault zones. Finally, discuss the challenges in fractured reservoir exploitation in deep tight carbonate rocks.

2. Geological and Exploitation Background

The Sichuan Basin is a large petroliferous basin in southwestern China [24]. It is a superimposed basin with multiple tectonic evolutions (Figure 1b) [24,25]. Its carbonate successions were deposited from the Ediacaran to early Triassic periods. Multiple carbonate sedimentary cycles overlap from the Ediacaran–Cambrian and Permian–Triassic periods throughout the basin [17]. The Ediacaran post-rift sedimentary successions unconformably overlap with the pre-Ediacaran crystalline basement. There is an intracratonic carbonate platform inherited from the Cambrian to Ordovician periods in the central basin. The central uplift was initiated in the late Ordovician period, with an absence of the Silurian–Carboniferous successions. The carbonate platform redeveloped from the middle Permian to middle Triassic periods and was unconformably overlain by late Triassic–Cretaceous siliciclastic rocks. A large number of siliciclastic rocks were denudated to form regional unconformities during the Indosinian–Yanshan movements. During the Himalayan movement, thrust-fold belts developed around the basin margins. With multiple shale source assemblages forming during early Cambrian, early Silurian, and Permian periods, carbonate reservoirs from the Ediacaran–Cambrian and Carboniferous–Triassic have become the major gas exploration and development domain in China [17,26].

The middle Permian–early Triassic carbonate successions developed along the Kaijiang-Liangping Trough in the northern Sichuan Basin (Figure 1). A southwest-trending depression was formed during the Permian extension [20]. The margins of this carbonate platform were initiated along the depression margins during the period of the Changxing Formation deposition and were gradually drowned during the Feixianguan Formation in the Early Triassic [18–21]. The carbonate platform margins developed from a gentle carbonate ramp to rimmed platform margin during the period of the Changxing Formation (Figure 1c). The Changxing reef–shoal microfacies developed along the platform margins, with a thickness of bioclastic and reef limestone more than 300 m. Large amounts of bioclastic shoals and interbedded sponge reefs were widely distributed along the platform margins [19–21]. A Permian reef–shoal reservoir developed along both sides of the platform margins [17–21]. However, in the ultra-deep subsurface, matrix reef–shoal reservoirs are generally of low porosity (<1 mD) and low permeability (<2 mD). Most of the porosity was lost by the carbonate cementation during the long burial diagenesis, which led to a low matrix porosity–permeability and strong heterogeneity [18–20]. It has been found that dolomitization, as well as penecontemporaneous and burial dissolution, are favorable for the improvement of secondary porosity [21,22]. Except for a few high-production gas wells, most production wells present a low and variable gas production in deep reservoirs. This suggests that these carbonate reservoirs are characterized by multi-porosity, strong hetero-

geneity, and variable productivity. Permian reef–shoal bodies along platform margins have been described using seismic technologies [27]. Recently, some NW-trending strike-slip faults were identified in the Kaijiang-Liangping Trough [23]. The width of the fault damage zone was up to 500 m using seismic description. In addition, the high-production wells were closely correlated with the fault damage zone. In this context, the fractured reservoirs along the strike-slip faults could be favorable new exploitation targets in this carbonate gas field.

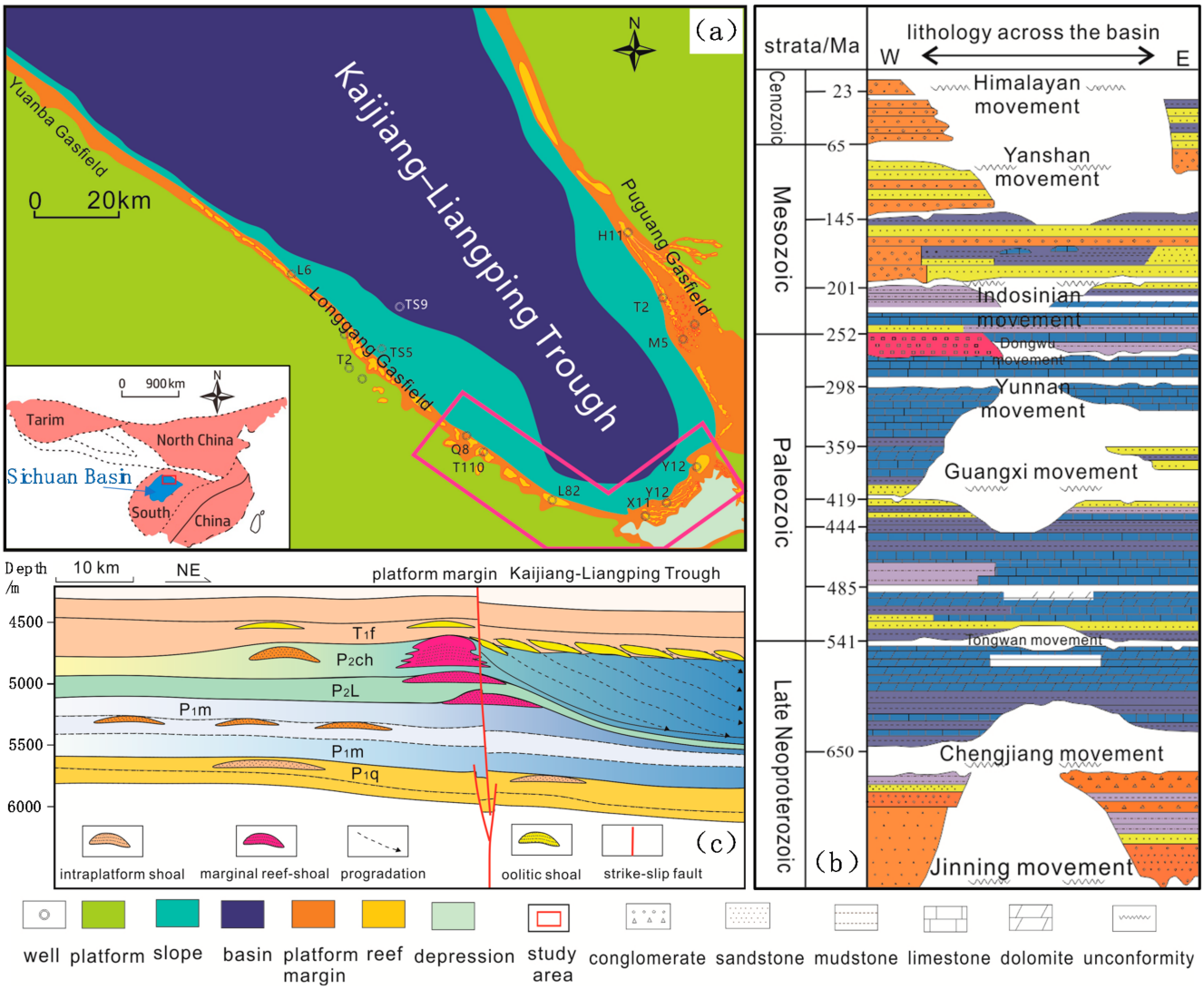

Figure 1. (**a**) Outline of the Kaijiang-Liangping Trough (Inset shows regional location), (**b**) the stratigraphic column, and (**c**) the geological section across the Permian–Triassic platform margin (after Reference [23]).

3. Data and Methods

More than 10,000 km^2 of 3D seismic surveys have been carried out along the Permian platform margins for purpose of carbonate exploration and development. Strike-slip faults have been identified in this study area, with the production of 1100 km^2 of 3D pre-stack time-migrated data. In the Permian carbonates, the seismic bin is 25 × 25 m, and the dominant frequency is in the range 30–40 Hz, both of which are favorable for fault mapping and reef–shoal description [23,27].

Furthermore, seismic attributes discovered using the steerable pyramid process have been used to identify fault damage zones [23]. The steerable pyramid process could divide the seismic data into several bandpass-filtered components with different directions, using

radial and planar filters in the FK domain. The amplitude attribute of the directional filtered data was used to describe the strike-slip fault damage zone [23]. In addition, the amplitude attribute had a positive correlation with the fractured reservoirs in the tight carbonate rocks [23]. Generally, seismic wave attenuation is highly sensitive to fractures in carbonate reservoirs [14,15]. In this way, the anisotropic energy utilized in the steerable pyramid process was used to describe the fractured reservoirs in the study area.

We collected the static and dynamic data of more than 30 production wells. Due to the sparsity of cores available for fractured reservoir analysis, we carried out FMI (formation microimager) processing of the fractured reservoirs in 10 wells. We compiled core and FMI data to describe the fractured reservoirs. In addition, we collected the physical properties of the cores, and interpreted logs to analyze their porosity and permeability. These measurements allowed us to arrive at a detailed analysis of the fractured reservoirs of the Permian carbonate.

Together with the geological, logging, and seismic data, we described the fractured reservoirs and correlated them with the strike-slip fault, in order to arrive at an analysis of the fracture effects on tight carbonate reservoirs.

4. Characteristics of the Faults and the Carbonate Reservoirs

4.1. Distribution of the Strike-Slip Faults and Reef–Shoal Bodies along the Platform Margin

In the study area, nine NW-trending strike-slip fault zones were identified using seismic data (Figure 2). The total length of the strike-slip fault zones in the study area is about 290 km. The strike-slip faults are parallel with each other and with the platform margin. They are segmented, with different types of echelon/oblique, soft-hard linked, and horsetail structure. In the seismic section (Figure 3), the strike-slip faults are developed in three tectonic layers of Lower Cambrian-Basement, Middle Cambrian–Carboniferous, and Permian–Triassic strata. Generally, the strike-slip faults are transtensional faults in the lower and upper tectonic layers, with transpressional faults in the middle tectonic layer. The faults are vertical and spread up to the upper strata, showing flower structures (negative and positive flower structure) in the seismic section. The multiple flower structures superimposed on the different tectonic layers suggest at least three stages of fault reactivation. In addition, the transtensional–transpressional–transtensional faults in the three layers indicate the existence of fault inversion during the fault activity.

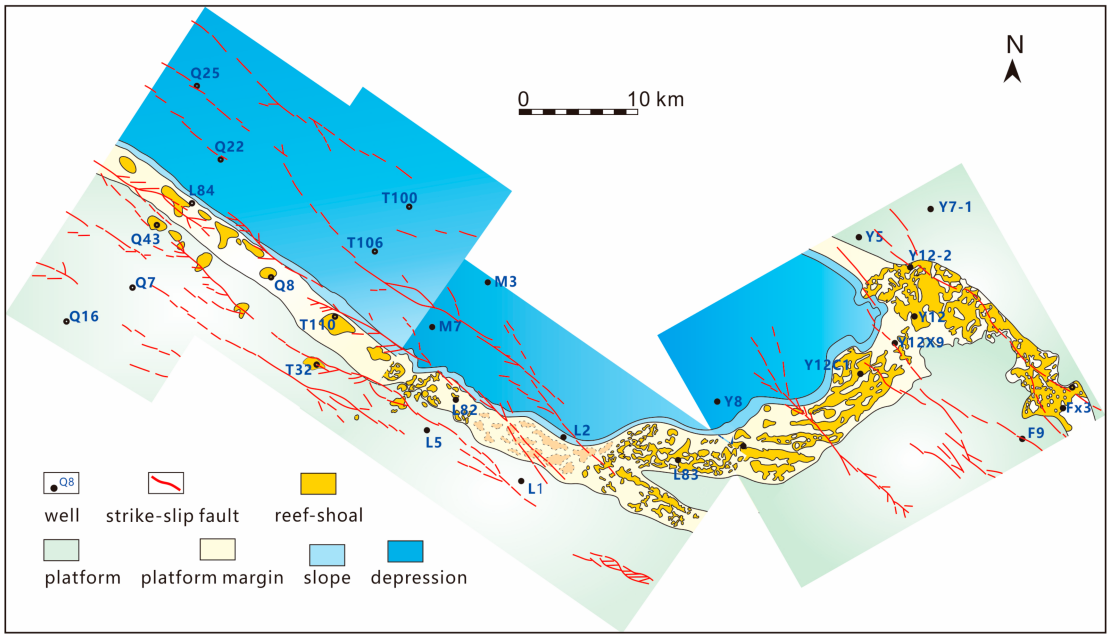

Figure 2. The strike-slip faults overlapping with the reef–shoal bodies in the Changxing Formation in eastern Kaijiang-Liangping area.

Calibrated using well lithofacies data, a strata isopach map was used to identify the reef–shoal bodies in the Changxing Formation (Figure 2). In the study area, the reef–shoal bodies in the Changxing Formation are mainly distributed along the platform margin. They are consistent with previous studies [17–21]. The high energy level of the reef–shoal bodies is closely related to localized paleogeomorphic heights. In the seismic section, the reef–shoal body generally presents a distinct mound shape, forming a rimmed platform margin. It was noted that there was a distinct strike-slip fault zone overlapping with the NW-trending platform margin. Two strike-slip fault zones intersected the northeastern platform margin and showed different reef–shoal body distributions in different zones. This suggested that the strike-slip fault had an effect on the reef–shoal distribution.

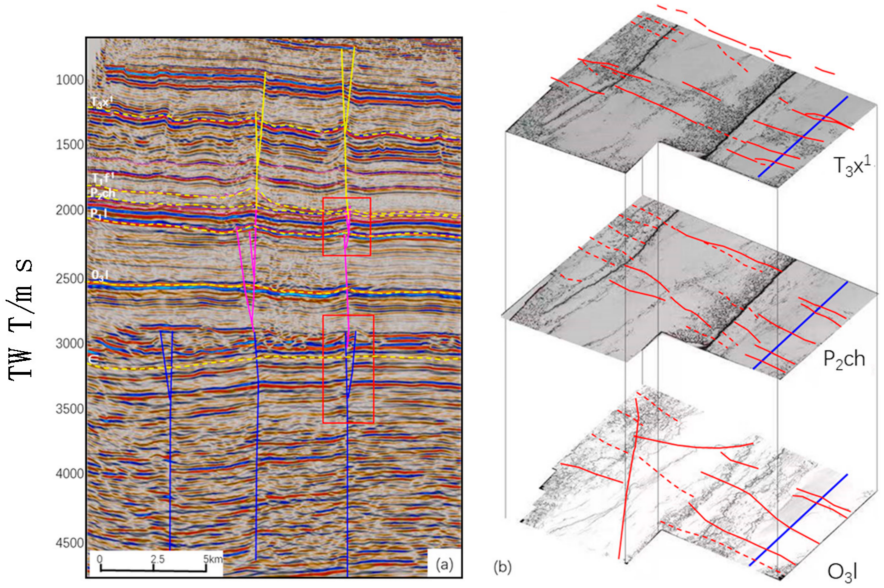

Figure 3. Typical seismic section showing three layered fault zones ((**a**); the blue, pink, and yellow lines showing the strike-slip faults in different layers; TWT: two-way travel time of seismic wave and different fault assemblages in different layers) and the strike-slip faults in three layers ((**b**); the red lines showing the strike-slip faults; the blue line showing the location of Figure 3a). T_3x^1: the Upper Triassic Xujiahe Formation; P_2ch: the upper Permian Changxing Formation; O_3l: the Upper Ordovician.

4.2. Analysis of Fractured Reservoirs Using Borehole Data

The reservoirs in the Changxing Formation are mainly reef–shoal bodies along the platform margins [17–22] (Figure 2). Most of the primary porosity in these reservoirs has been occluded by intense cementation during their long burial history (Figure 4d–f). More than 80% of the porosity is secondary dissolution of the pore and vug (diameter between 2–100 mm) (Figure 4). The fracture network is developed in the fault damage zone. Moreover, the fracture-related dissolution porosity is common in the cores and thin sections (Figure 4c,f). In the fractured reservoirs, most fractures present high angles and narrow apertures, whereas there are multiple set fractures with high and low dips, which form a complicated fracture network in the fault zone. A few wells have penetrated breccias in the fault damage zone (Figure 4b). The well T110 presented a system of complicated fracture–cave reservoirs (cave diameter >100 mm) in the logging data.

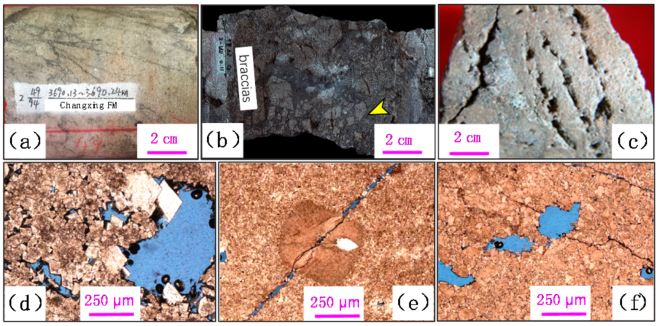

Figure 4. Photographs of the Permian carbonate reservoirs. (**a**) high dip fracture network, T110, 3690 m, core; (**b**) breccias in the fault damage zone, Q42, 4901 m, core; (**c**) dissolution pores and vugs along fractures, F3, 4884 m, core; (**d**) intercrystalline dissolution pores in the dolomite, T110, 4337.12 m, thin section; (**e**) opened fracture across the bioclastic dolomite, F3, 4884.07 m, thin section; (**f**) oblique fractures and dissolution pores, T2, 3859.60 m, thin section.

The matrix porosity of the Ediacaran carbonates is generally less than 5%, and the permeability is generally less than 0.5 mD (Figure 5). Whatever the lithology, the permeability is extremely low in the dissolution reservoirs. Hence, the matrix reservoirs have shown a low gas production. The fracture porosity is generally less than 0.1%, but fracture-related dissolution porosity was seen to develop in the fault zones. The porosity can increase multiple times in the fractured reservoirs. The porosity is up to 5–11%, through dissolution pores being developed along the fracture zones (Figure 5a). Furthermore, the permeability can increase from 1 to 2 orders of magnitude in the fault zone (Figure 5b). The fracture reservoirs present a permeability of more than 5 mD. Importantly, the pore throats are micro-throats (radius <0.1 μm) in the matrix reservoirs but are more than 5 μm in the fracture samples. Generally, the gas production in the matrix reservoirs is generally lower than 200,000 m^3/d. Whereas the high-production wells penetrated into the fractured reservoirs and the gas production yielded was from 400,000 up to 1,200,000 m^3/d (Figure 5c). During the well drilling process, the fractured reservoirs presented mud leakage and drill breakage. The gas production data also present a power-law distribution, which is related to the distance to the fault core. When the distance to the fault is more than 1300 m, the gas production presents a sharp decrease with increasing distance. This is consistent with the porosity and permeability data. It is noted that many lower permeability and porosity reservoirs were also found in the fault zone. These led to a large scattered distribution within the fault damage zone. These porosities form two kinds of reservoir, ranging from the low permeability of the tight matrix reservoirs, to highly permeable fractured reservoirs. In this context, carbonate reservoirs are extremely heterogeneous, and the physical properties of the reservoirs vary greatly in the vertical and horizontal directions.

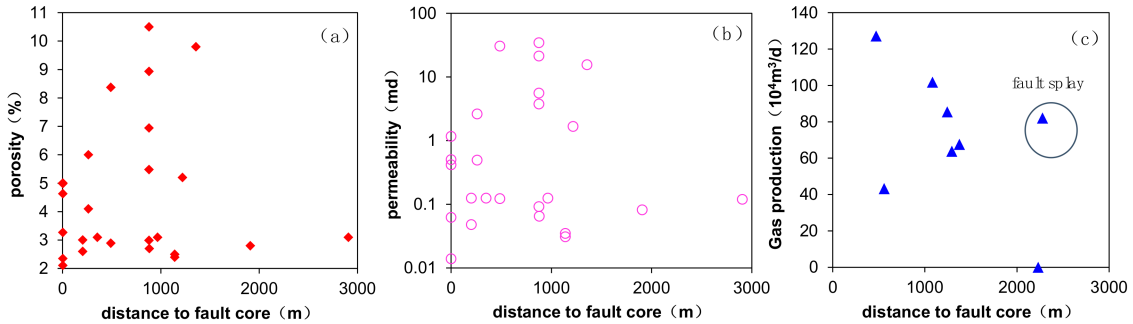

Figure 5. Porosity (**a**), permeability (**b**), and gas production (**c**) vs. distance to the fault in the Permian reservoirs.

4.3. Seismic Description of the Fractured Reservoirs

It has been suggested that the seismic characteristics of steerable pyramid processing are favorable for the identification of fault damage zones alongside strike-slip fault zones [23]. Considering that seismic wave attenuation and anisotropy are highly sensitive to fractures in carbonate reservoirs [14,15], we selected the anisotropic energy attribute of the steerable pyramid process to describe the fractured reservoirs (Figure 6). Although microfractures cannot be identified from seismic data, the boundaries of the fault damage zone can be imaged using amplitude. Strong energy anisotropy is consistent with the fault damage zone. The strength of the anisotropic energy parameter can be used as a proxy for the strength of fractured reservoirs.

The results indicated the varied strength of the fractured reservoirs in the plane and section of the fault zone. The width of a fault damage zone was up to 600 m in the Permian carbonate. In the overlapping and intersection zones, the width of the fault damage zone was more than 2 km. This is consistent with the porosity and permeability distribution (Figure 5). Similarly to the porosity and permeability, there was a decreasing trend of anisotropic energy values with increasing distance from the fault (Figure 7a). Meanwhile, the seismic parameter indicated the strong heterogeneity of the fractured reservoirs in the fault zone. This is consistent with the tighter reservoirs in the fault damage zones, which could be related to the stronger diagenesis and filling of the fractured porosity. In this way, there was a large range of levels of gas production in the fault zones. The high production areas were closely correlated to the seismic activity (Figure 7b), suggesting highly permeable reservoirs and a heterogeneous dissolution porosity developed in the fault damage zone. The high-production wells are close to the fault core, within a distance of 1300 m, and have penetrated the "sweet spots" of the fractured reservoirs. It is noted that many high-production wells in the fractured reservoirs showed a rapid decline in production during the production period.

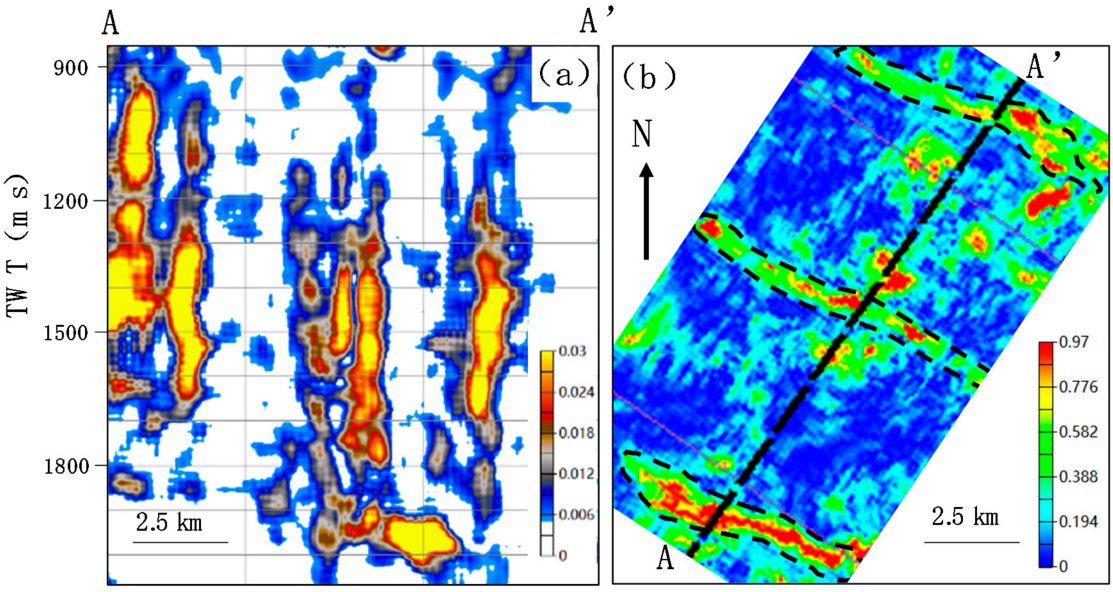

Figure 6. The strong anisotropic energy, showing the fractured reservoirs of the fault zones in the study area in a section (**a**) and in a planar plot (**b**) (the orange block shows the fractured reservoirs along the fault zone).

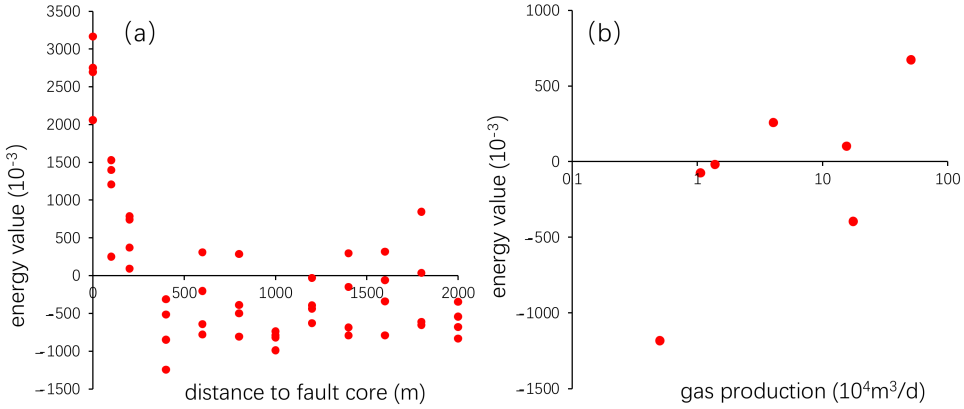

Figure 7. Energy value from anisotropic energy vs. distance to fault core (**a**) and vs. gas production (**b**) in the carbonate platform margin.

4.4. Aplication in Deep Reservoir Exploitation

Through the borehole data investigation, it was seen that well T110 had penetrated the fractured reservoir in the fault zone (Figure 8). This well is located in the inner fault damage zone, and runs along the carbonate platform margin. The strike-slip fault has inherited fault activity from the Permian to the Triassic, which has led to the width of the fault damage zone being more than 500 m in the reef–shoal body. Fracture networks and breccias were well developed in the cores and the logging images. The fractures developed with a main NW-trend with a fracture frequency of up to 5/m. The dissolution porosity was found along the fracture and its adjacent grainstone, forming fracture–vugs and fracture–cave reservoirs. High porosity (4–9%) mainly occurred in the fractured section. Gas invasion and abnormal gas was shown in the fractured reservoirs. As a result, the gas production was up to 580,000 m^3/d, which is much higher than the gas production of 156,000 m^3/d that was achieved with the matrix reservoir in the adjacent well Q8 (Figure 8). This suggests that fractured reservoirs in the strike-slip fault zone could be a "sweet spot" for high levels of gas production in deep gas field exploitation.

Using seismic reservoir description, the horizontal well Y12C1 was drilled to penetrate the fractured reservoir (Figure 9). The well was optimized for the reef–shoal reservoir zone overlapping with the fault damage zone. Although the small fault was ambiguous in the conventional seismic section, the "sweet spot" of the fractured reservoir could be imaged using the seismic attribute. The Y12C1 well has a drilling direction going from the inner to the outer of the fault damage zone. The well penetrated the outer damage zone, with several sets of fracture zones and dissolution pores and vugs. The well had a mud loss of 1904 m^3 during drilling. The gas production was up to 1,180,000 m^3/d in the fractured reservoirs. This suggests, on the one hand, that the fractured reservoir had developed along the small strike-slip fault zone, although there was weak seismic response in the seismic section and planar attribute. On the other hand, this may well indicate a wider fault damage zone in the fault zone.

As a result of our research, we feel confident in saying that the fault damage zone is favorable for the development of the "sweet spots" of the fractured reservoirs. The amplitude parameter could be used for reservoir description of a deep fractured reservoir. The abnormal energy (orange-red spots in Figure 6) indicated the "sweet spots" of fractured reservoirs along the fault damage zone. Considering the uncertainty of the seismic data, the calibration of wells could be helpful for constraining the boundary and strength of the fractured zone. In addition, efficient well location has always been associated with "positive landform, and the presence of abnormal seismic attributes in intense fault damage zones".

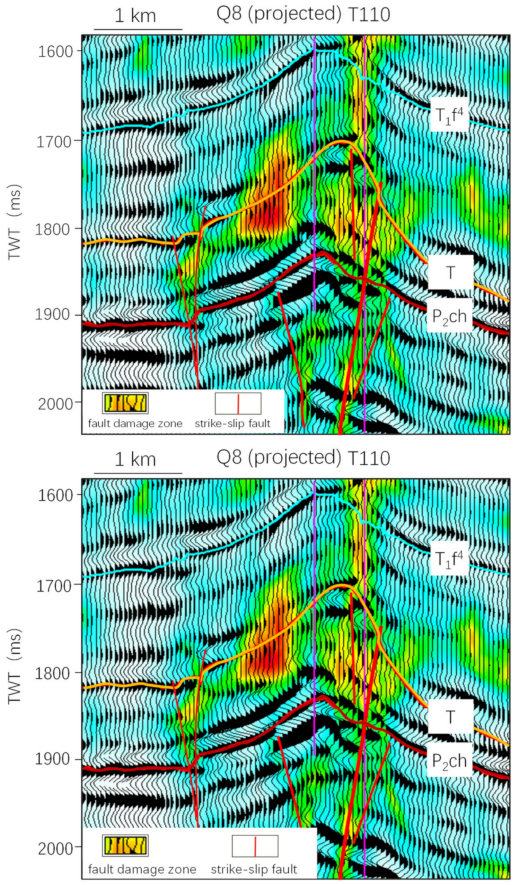

Figure 8. Seismic section with the energy parameter (green-orange color), showing the fault damage zone overlapping the reef–shoal along the Permian platform margin (T_1f^4: the fourth member of the Lower Triassic Feixianguan Formation; P_2ch: the upper Permian Changxing Formation).

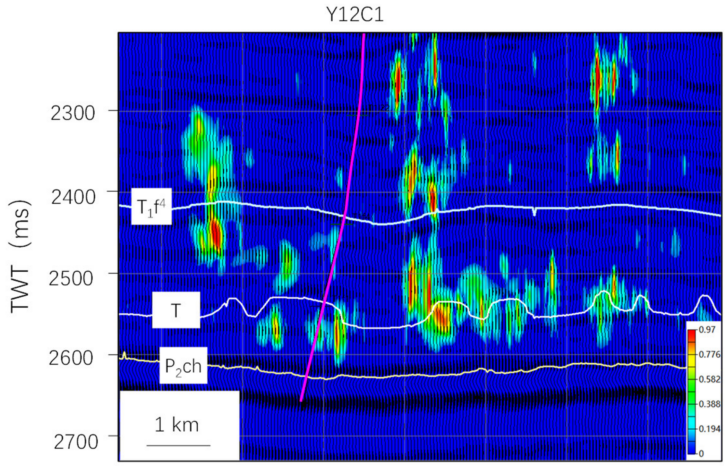

Figure 9. Seismic section with energy (green-orange color) across well Y12C1 (the green-orange blocks indicate the fault damage zone).

5. Discussion

5.1. Fracture Effects on the Carbonate Reservoir

In the reservoir evaluation of the production wells, the "sweet spot" fractured reservoirs occurred at different positions along the strike-slip fault zones. The carbonate fault damage zone varied greatly along the strike, showing distinct heterogeneity (Figures 6 and 9). At the peripheries, the fault damage zones are narrow and have a weak seismic response. The width of the damage zone increases towards the middle part of the segment, especially the

width of the damage zone at the top of the fractured reservoirs, which is much wider than expected when considering the size of the displacement itself [28]. This may be related to fault overlapping and branch growth, and it may also be related to the intense fracturing and karstification at the top of the carbonate reservoirs [29]. Regarding the seismic profiles, the fault damage zone becomes complex, with fault splays developing at the lower part of the fault zone, which cause a multi-stage superposition of fracturing. Away from the tip of the fault damage zones, horsetail structures appear to form a widely fractured area.

Generally, the high-energy microfacies are assumed to be the main controlling factors in the development of carbonate reservoirs [17–22]. Although the reef–shoal reservoirs are well developed in the deep Permian carbonate platform margin (Figure 2), the matrix reservoirs mainly have low porosity (<4%) and permeability (<0.5 mD) (Figure 5). This is comparable to the deep tight reservoirs found globally [30]. Studies have shown that the ancient carbonate reservoirs experienced a long diagenesis and have lost almost all of their primary porosity, now showing secondary dissolution porosity [19–22]. High-production wells generally occur along strike-slip fault zones. The data suggested that fracturing plays an important role in the development of secondary porosities, particularly of the "sweet spots" of fractured reservoirs.

Statistical data suggested that fracture networks are more likely to develop along fault damage zones that are more than 1000 m in width. The effective fracture porosity in a matrix reservoir is generally lower than 0.1%, but the dissolution porosity along the fracture can increase more than twice when moving along the fault damage zone. Furthermore, fracturing plays an important role in controlling the permeability of tight carbonate rocks. The matrix permeability of carbonate rocks in cores is generally lower than 0.5 mD, but the permeability of fractured samples in core generally varies in a range of 0.1–100 mD, which may be increased by 1–3 orders of magnitude. According to the analysis of the logging interpretation, the permeability of a fractured reservoir can increase by 1–2 orders of magnitude (Figure 5). High-energy reef–shoal reservoirs are generally of extremely low porosity and permeability, which leads to low gas production. In the carbonate fault damage zone, the fracture–vug and fracture–cave reservoirs have a relatively higher porosity (>5%) and a much higher permeability (>10 mD). Seismic reservoir description showed that fractured reservoirs developed within 1300 m of the fault cores and, in particular, within 500 m of the area of fault damage zones.

The influence of sedimentary facies and karstification on the strike-slip fault zone present two kinds of reef–shoal reservoir and fractured reservoir. It is noted that the fractured reef–shoal reservoir is the favorable "sweet spot" for high and stable gas production. In this way, the uniform well pattern utilized in conventional development methods cannot realize the localized "sweet spot" of fractured reservoir development in a deep tight matrix reservoir.

5.2. Distribution of Fractured Reservoirs

As seen in multiple overprints of tectonic activity, the fault cores in carbonates usually have a complicated deformation with varied fault rocks. Generally, carbonate breccias and cataclastic rocks are found in the fault cores. Furthermore, there are intense fillings of multiple secondary calcite cements and veins, as well as gouging from the overlain strata, which occurs in the complicated deformation zone. Whereas many fault cores have open fractures and dissolution porosity in the small fault zones, this is different from the fault zones in typical carbonate rocks [29,31]. This could be related to the relatively small number of faults in these studies that had a low fault maturity and few fillings (Figure 4). Fracture networks develop along fault damage zones, which are generally abnormal and highly permeable structures. The outer damage zone generally has fewer fracture frequencies than the inner zone, although it is difficult to identify its boundary within the inner zone and the host rocks in the data.

The fracture elements generally show a significant power-law distribution, commensurate with their distance from the fault cores, which is consistent with the porosity and

permeability distribution pattern of Ordovician carbonate rocks in the strike-slip fault zone of the Tarim Basin [28] and fault elements in other places [29]. As the intraplatform shoal reservoirs were overlapped by strike-slip fracturing, high-quality fracture–vug reservoirs developed along the strike-slip fault damage zones through the process of fracture-related karstification. The three elements of microfacies, faults, and dissolution controlled the development and distribution of high-quality reservoirs. In this way, the relatively higher matrix porosity is significantly improved by the fracturing and by the related dissolution.

In the study area, the matrix reef–shoal reservoirs were widely distributed along the platform margin, but the "sweet spots" of fractured reservoirs occurred only in localized damage zones. Localized fractured reservoirs are the main targets for high levels of production. The distribution of "sweet spots" in the fractured reservoirs is variable in the strike–slip fault damage zone (Figure 6). Besides their abnormally high porosity and permeability values (Figure 5), the fractured reservoirs also present a power-law that gradually decreases across the strike-slip fault zone, whereas there is a distinct scattering of data gathered from the fault zone that is far away from the typical power-law distribution (Figure 5). In fact, these much lower porosity–permeability values and lower production data are correlated with the negative effects of the fault activity. Fault gouging and cementation also occurred in the fault damage zone. Structural diagenesis could have been the reason for the decrease in the porosity and permeability of the fractured reservoir, occurring over the course of its long burial history.

Generally, seismic anisotropy and geometry-based methods are used in the description of fractured reservoirs [32,33]. Considering that seismic wave attenuation and anisotropy are highly sensitive to fractures in carbonate reservoirs [14,15,34,35], the anisotropic energy steerable pyramid process is favorable for description of deep subsurface fractured reservoirs (Figures 6–9). In the study area, the large-scale fractured reservoirs were scattered along the fault damage zone with chaotic seismic reflection and strong wave attenuation. This is consistent with the fractured reservoirs from borehole data. However, the quantitative description of fractured reservoirs using the low-resolution seismic data in the deep subsurface remains a challenge. Furthermore, the boundary of the fractured reservoir is difficult to discriminate using seismic energy.

6. Conclusions

1. Reef–shoal reservoirs generally have a tight matrix porosity and low production level in the deep Permian carbonate rocks.
2. Porosity, permeability, and gas production have an increasing trend, from the country rocks to the strike-slip fault core. The porosity along the fault damage zone can increase more than once and the permeability can be increased by 1–2 orders of magnitude.
3. Anisotropic energy is favorable for the description of fractured reservoirs in the fault damage zone, suggesting a strong heterogeneity of the fractured reservoirs in the fault zone.
4. The "sweet spots" of fractured reservoirs, which were found to be widely developed along the small-scale strike-slip fault zones, are favorable for high hydrocarbon production in deep subsurface tight matrix reservoirs.

Author Contributions: Conceptualization, X.L. and G.W.; methodology, J.L., and L.F.; software, S.L. and L.F.; investigation, X.L. and S.C.; data curation, S.C. and Y.W.; writing—original draft preparation, G.W. and X.L.; visualization, J.L. and L.F.; supervision, B.L. and F.L.; funding acquisition, F.L. and B.L. All authors have read and agreed to the published version of the manuscript.

Funding: The technology project of PetroChina Southwest Oil & Gasfield Company (JS2022-025), the Science and Technology Cooperation Project of the CNPC-SWPU Innovation Alliance (2020CX010101) and the National Natural Science Foundation of China (41972121).

Data Availability Statement: Not applicable.

Acknowledgments: The authors are grateful to the reviewers and editors for their constructive comments and suggestions that substantially improved the manuscript. The authors also thank Xihui Xu, Xiaojun Zhou, Shuhang Tang, Shuai Yang and Bingshan Ma for their help in the data process.

Conflicts of Interest: The authors declare no conflict of interest.

References

1. Akbar, M.; Vissapragada, B.; Alghamdi, A.H.; Allem, D.A. Snapshot of carbonate reservoir evaluation. *Oilfield Rev.* **2000**, *12*, 20–21.
2. Garland, J.; Neilson, J.; Laubach, S.E.; Whidden, K.J. Advances in carbonate exploration and reservoir analysis. *Geol. Soc. London Spec. Publ.* **2012**, *370*, 1–15. [CrossRef]
3. Zou, C.N.; Zhai, G.M.; Zhang, G.Y.; Wang, H.J.; Zhang, G.S.; Li, J.Z.; Wang, Z.M.; Wen, Z.X.; Ma, F.; Liang, Y.B.; et al. Formation, distribution, potential and prediction of global conventional and unconventional hydrocarbon resources. *Pet. Explor. Dev.* **2015**, *42*, 13–25. [CrossRef]
4. Guo, X.S.; Hu, D.F.; Li, Y.P.; Duan, J.B.; Zhang, X.F.; Fan, X.J.; Duan, H.; Li, W.C. Theoretical Progress and Key Technologies of Onshore Ultra-Deep Oil/Gas Exploration. *Engineering* **2019**, *5*, 458–470. [CrossRef]
5. Zhang, G.Y.; Ma, F.; Liang, Y.B.; Zhao, Z.; Qin, Y.Q.; Liu, X.B.; Zhang, K.B.; Ke, W.L. Domain and theory-technology progress of global deep oil & gas exploration. *Acta Pet. Sin.* **2015**, *36*, 1156–1166. (In Chinese with English abastract)
6. Wang, Q.H.; Zhang, Y.T.; Xie, Z.; Zhao, Y.W.; Zhang, C.; Sun, C.; Wu, G.H. The advance and challenge of seismic technique on the ultra-deep carbonate reservoir exploitation in the Tarim Basin, Western China. *Energies* **2022**, *15*, 7653. [CrossRef]
7. He, X.; Guo, G.; Tang, Q.; Wu, G.; Xu, W.; Ma, B.; Huang, T.; Tian, W. The advances and challenges of the Ediacaran fractured reservoir development in the central Sichuan Basin, China. *Energies* **2022**, *15*, 8137. [CrossRef]
8. Wu, G.H.; Zhao, K.Z.; Qu, H.Z.; Nicola, S.; Zhang, Y.T.; Han, J.F.; Xu, Y.F. Permeability distribution and scaling in multi-stages carbonate damage zones: Insight from strike-slip fault zones in the Tarim Basin, NW China. *Mar. Pet. Geol.* **2020**, *114*, 104208. [CrossRef]
9. Liu, G.P.; Zeng, L.B.; Han, C.Y.; Ostadhassan, M.; Lyu, W.Y.; Wang, Q.Q.; Zhu, J.W.; Hou, F.X. Natural fractures in carbonate basement reservoirs of the Jizhong Sub-Basin, Bohai Bay Basin, China: Key aspects favoring oil production. *Energies* **2020**, *13*, 4635. [CrossRef]
10. Al-Gosayir, M.; Babadagli, T.; Leung, J.; Al-Bahlani, A.M. In-situ recovery of heavy-oil from fractured carbonate reservoirs: Optimization of steam-over-solvent injection method. *J. Pet. Sci. Eng.* **2015**, *130*, 77–85. [CrossRef]
11. Shafiei, A.; Ahmadi, M.A.; Dusseault, M.B.; Elkamel, A.; Zendehboudi, S.; Chatzis, I. Data analytics techniques for performance prediction of steamflooding in naturally fractured carbonate reservoirs. *Energies* **2018**, *11*, 292. [CrossRef]
12. Harimi, B.; Masihi, M.; Mirzaei-Paiaman, A.; Hamidpour, E. Experimental study of dynamic imbibition during water flooding of naturally fractured reservoirs. *J. Pet. Sci. Eng.* **2019**, *174*, 1–13. [CrossRef]
13. He, X.; Wang, R.; Yang, J.; Li, S.; Yan, C.; Wu, G. Optimization of oil productivity from the ultra−depth strike−slip fault−controlled carbonate reservoirs in northwestern China. *Energies* **2022**, *15*, 3472. [CrossRef]
14. Matsushima, J.; Mohammed, Y.A.; Bouchaala, F. A novel method for separating intrinsic and scattering attenuation for zero-offset vertical seismic profiling data. *Geophys. J. Intern.* **2017**, *211*, 1655–1668. [CrossRef]
15. Bouchaala, F.; Ali, M.Y.; Matsushima, J.; Bouzidi, Y.; Takam Takougang, E.M.; Mohamed, A.A.; Sultan, A. Scattering and intrinsic attenuation as a potential tool for studying of a fractured reservoir. *J. Pet. Sci.* **2019**, *174*, 533–543. [CrossRef]
16. Wang, R.J.; Yang, J.P.; Chang, L.J.; Zhang, Y.T.; Sun, C.; Wu, G.H.; Bai, B.C. 3D modeling of fracture-cave reservoir from an ultra−depth strike−slip fault−controlled carbonate oilfield in Northwestern China. *Energies* **2022**, *15*, 6415. [CrossRef]
17. Yang, Y.; Wen, L.; Xie, J.R.; Luo, B.; Huang, P.H.; Ran, Q.; Zhou, G.; Zhang, X.H.; Wang, H.; Tian, X.W.; et al. Progress and direction of marine carbonate gas exploration in Sichuan Basin. *China Pet. Explor.* **2020**, *25*, 44–55. (In Chinese with English abstract)
18. Zhang, J.Y.; Zhou, J.G.; Hao, Y.; Wang, X.F.; Lv, Y.Z.; Zhang, D.Z.; Xu, M.R.; Zhang, R.H.; Gu, M.F.; Zhang, J.Y. A Sedimentary model of Changxing and Feixianguan reservoirs around Kaijiang-Liangping Trough in Sichuan Basin. *Mar. Origi. Pet. Geol.* **2011**, *16*, 45–54.
19. Yang, Y.; Zhong, Y.; Li, L.J. Distribution and gensis of Permian-Triassic reef-shoal combination around Kaijiang-Liangping trough in Sichuan Basin, China. *J. Chengdu Univ. Technol.* **2021**, *48*, 683–690. (In Chinese with English abstract)
20. Wen, L.; Zhang, Q.; Yang, Y.; Liu, H.Y.; Che, Q. Factors controlling reef-bank reservoirs in the Changxing-Feixianguan formation in the Sichuan Basin and their play fairways. *Nat. Gas Ind.* **2012**, *32*, 39–44. (In Chinese with English abstract)
21. Su, C.P.; Tan, X.C.; Liu, H.; Tang, H.; Li, H.W.; Wang, G.F.; Tang, X.S.; Zhang, Q.Y.; Liao, Y.S. Characteristics and diagenesis of platform margin reef-shoal reservoirs of Upper Permian Changxing Formation around Kaijiang-Liangping Trough, eastern Sichuan Basin. *Geol. China* **2016**, *43*, 2046–2058.
22. Feng, L.J.; Jiang, Y.Q.; Liu, F.; Gu, Y.F.; Wang, Z.L.; Zhong, K.X.; Liao, Y.S. Reservoir characteristics and main controlling factors of oolitic shoal reservoir in Feixianguan Formation in the southern part of Kaijiang-Liangping trough, eastern Sichan Basin. *Acta Pet. Sin.* **2021**, *42*, 1287–1298. (In Chinese with English abstract)
23. Tang, Q.; Tang, S.; Luo, B.; Luo, X.; Feng, L.; Li, S.; Wu, G. Seismic description of deep strike-slip fault damage zone by steerable pyramid method in the Sichuan Basin, China. *Energies* **2022**, *15*, 131. [CrossRef]

24. He, D.; Li, D.; Zhang, G.; Zhao, L.; Fan, C.; Lu, R.; Wen, Z. Formation and evolution of multi-cycle superposed Sichuan Basin, China. *Chin. J. Geol.* **2011**, *46*, 589–606. (In Chinese with English abstract)
25. Li, H.K.; Li, Z.Q.; Long, W.; Wan, S.S.; Ding, X.; Wang, S.Z.; Wang, Q.Z. Vertical configuration of Sichuan Basin and its superimposed characteristics of the prototype basin. *J. Chengdu Univ. Technol.* **2019**, *46*, 257–267. (In Chinese with English abstract)
26. Zou, C.N.; Du, J.H.; Xu, C.C.; Wang, Z.C.; Zhang, B.M.; Wei, G.Q.; Wang, T.S.; Yao, G.S.; Deng, S.H.; Liu, J.J.; et al. Formation, distribution, resource potential and discovery of the Sinian−Cambrian giant gas field, Sichuan Basin, SW China. *Petrol. Explor. Dev.* **2014**, *41*, 306–325. [CrossRef]
27. Gong, X.X.; Yang, W.; Li, W.J.; Zhou, X.G.; Tang, Q.S.; Zhang, J. Characteristics and geological properties of seismic bright spots in the Permian carbonate deposit, Changhsing Formation, Longgang Area, Northeast Sichuan Basin, China. *Carbon. Evapor.* **2020**, *35*, 98. [CrossRef]
28. Torabi, A.; Berg, S.S. Scaling of fault attributes: A review. *Mar. Petrol. Geol.* **2011**, *28*, 1444–1460. [CrossRef]
29. Wu, G.H.; Gao, L.H.; Zhang, Y.T.; Ning, C.Z.; Xie, E. Fracture attributes in reservoir-scale carbonate fault damage zones and implications for damage zone width and growth in the deep subsurface. *J. Struct. Geol.* **2019**, *118*, 181–193. [CrossRef]
30. Nelson, P.H. Pore-throat sizes in sandstones, tight sandstones, and shales. *AAPG Bull.* **2009**, *93*, 329–340. [CrossRef]
31. Agosta, F.; Ruano, P.; Rustichelli, A.; Tondi, E.; Galindo-Zaldívar, J.; Sanz de Galdeano, C. Inner structure and deformation mechanisms of normal faults in conglomerates and carbonate grainstones (Granada Basin, Betic Cordillera, Spain): Inferences on fault permeability. *J. Struct. Geol.* **2012**, *45*, 4–20. [CrossRef]
32. Benmadi, M.; Sayantan, G.; Roger, S.; Kurt, M.; Mashhad, F. Practical aspects of upscaling geocellular geological models for reservoir fluid flow simulations: A case study in integrating geology, geophysics, and petroleum engineering multiscale data from the Hunton Group. *Energies* **2020**, *13*, 1604. [CrossRef]
33. Babasafari, A.A.; Chinelatto, G.F.; Vidal, A.C. Fault and fracture study by incorporating borehole image logs and supervised neural network applied to the 3D seismic attributes: A case study of pre-salt carbonate reservoir, Santos Basin, Brazil. *Pet. Sci. Techn.* **2022**, *40*, 1492–1511. [CrossRef]
34. Yang, Y.; Yin, X.; Zhang, B.; Cao, D.; Gao, G. Linearized frequency-dependent Reflection coefficient and attenuated anisotropic characteristics of Q-VTI model. *Energies* **2021**, *14*, 8506. [CrossRef]
35. Bouchaala, F.; Ali, M.Y.; Matsushima, J.; Bouzidi, Y.; Jouini, M.S.; Takougang, E.M.; Mohamed, A.A. Estimation of seismic wave attenuation from 3D seismic data: A case study of OBC data acquired in an offshore oilfield. *Energies* **2022**, *15*, 34. [CrossRef]

Disclaimer/Publisher's Note: The statements, opinions and data contained in all publications are solely those of the individual author(s) and contributor(s) and not of MDPI and/or the editor(s). MDPI and/or the editor(s) disclaim responsibility for any injury to people or property resulting from any ideas, methods, instructions or products referred to in the content.